ELSEVIER

Journal of Nuclear Materials 290–293 (2001) 1138–1143

journal of nuclear materials

www.elsevier.nl/locate/jnucmat

Vertical target and FW erosion during off-normal events and impurity production and transport during ELMs typical for ITER-FEAT

H. Würz [a,*], S. Pestchanyi [b], B. Bazylev [c], I. Landman [b], F. Kappler [a]

[a] *Forschungszentrum Karlsruhe, Institut für Hochleistungsimpuls- und Mikrowellentechnik, Postfach 36 40, D-76021 Karlsruhe, Germany*
[b] *Troitsk Institute for Innovation and Fusion Research, 142092 Troitsk, Russian Federation*
[c] *Luikov Institute of Heat and Mass Transfer, 280008 Minsk, Belarus*

Abstract

During off-normal events besides evaporation macroscopic erosion might occur. In carbon-based materials (CBMs) macroscopic erosion means brittle destruction and dust formation and in metals melt layer motion and droplet splashing. Dust, melt flow, droplet splashing and redeposited evaporated material produce complex layers with considerable surface roughness and drastically reduced heat conductivity. Moreover flaking and easy levitation of particles might occur. Subsequent ELMs when depositing their energy into such layers might enhance impurity production because of increased heating of the hot spots. For vertical targets and for first walls (FWs) macroscopic erosion is analyzed. For a simplified hot spot scenario a first estimation on maximum tolerable ELM energy is given. © 2001 Elsevier Science B.V. All rights reserved.

Keywords: Disruption; Plasma shield; Impurity transport; Erosion; ELM

1. Introduction

This paper gives a comprehensive discussion of vertical target and first wall (FW) damage for the off-normal events listed in Table 1. Graphite and tungsten are considered as vertical target and beryllium and tungsten as FW material. Damage mechanisms considered are evaporation and brittle destruction of graphite [1], melting, melt motion [2] and droplet splashing due to boiling and bubble collapse and due to the onset of a Kelvin Helmholtz (KH) instability with growing surface waves for metals. Triggered by the observation of giant ELMs at JET, in which up to 10% of the plasma thermal energy content was dumped to the divertor [3], the problem of divertor erosion during ITER-type I ELMs was addressed recently [4]. However another problem related with ELMs could be the enhanced impurity production in redeposited layers with drastically reduced heat conductivity. Moreover the surface roughness and the easy levitation of particles from the redeposited layer result in increased energy deposition into hot spots. The impurity production for such a complex situation has to be estimated and the maximum tolerable energy deposited during an ELM has to be specified.

2. Brittle destruction of graphite

2.1. Simulation experiments

The estimations on brittle destruction are based on the threshold energy of 10 kJ g^{-1} which was derived from e-beam experiments [1]. Fig. 1 shows a comparison of the measured and calculated total mass loss (evaporation and brittle destruction) for CFC graphite for the JEBIS facility [5] with perpendicular impact of 70 keV electrons of peak target heat load of 1.8 GW m^{-2} and

* Corresponding author. Tel.: +49-07247 825987; fax: +49-07247 825987.
E-mail address: wuerz@ihm.fzk.de (H. Würz).

0022-3115/01/$ - see front matter © 2001 Elsevier Science B.V. All rights reserved.
PII: S0022-3115(00)00478-5

Table 1
Off normal events used for damage analysis and impurity production at vertical targets and FWs in ITER-FEAT

Type of event	Location	Energy density (MJ m^{-2})	Time duration (ms)	Target heat load used in analysis		Impact energy (keV)	Type of particles
				GW m^{-2}	(ms)		
Thermal disruption	Vertical target	30	$\leqslant$10	30	1	10	Hot plasma
				3	10		
ELMS	Vertical target	0.5	$\leqslant$1.0	1	0.5	3	Hot plasma
RAEs	FW	50	$\leqslant$50	0.5–2.5	20–100	Up to 20 MeV electrons	
VDEs	FW	50	100	0.5	100	$\leqslant$3 keV	Hot plasma

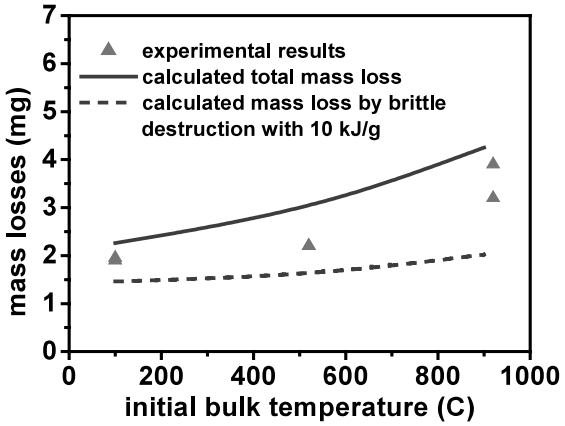

Fig. 1. Total mass loss for CFC graphite for JEBIS conditions with 70 keV e-beam, peak power pulse duration 20 ms, absorbed heat flux 1.8 GW m^{-2}.

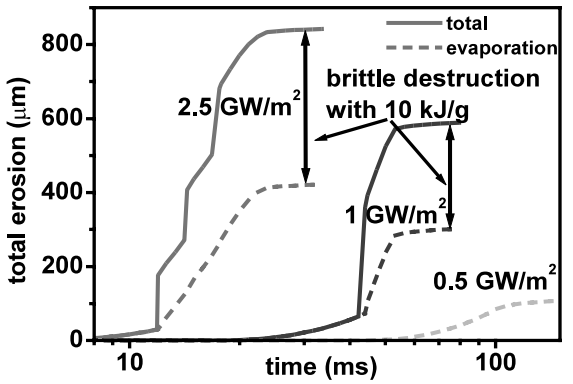

Fig. 2. Total erosion and evaporation of CFC graphite for 15 MeV RAEs with 50 MJ m^{-2}. The inclination angle of the RAEs is 1°.

2 ms pulse duration. Included is the calculated mass loss due to brittle destruction. A mass loss of 1 mg corresponds to an erosion depth of 65 μm. The size of the dust particles typically is a few microns.

In plasma gun experiments with surface energy deposition peak power densities up to 350 GW m^{-2} were used to initiate and investigate brittle destruction in graphite [6]. Dust particles have been detected. However the fraction of the eroded material which is due to brittle destruction is still unknown.

2.2. Tokamak conditions

Numerical results on total erosion and brittle destruction under RAE impact of energy density of 50 MJ m^{-2}, impact energy of 15 MeV and inclination angle of 1° are shown in Fig. 2 for CFC graphite for different target heat loads and a damage threshold energy value of 10 kJ g^{-1}. For 0.5 GW m^{-2} the specific energy within 100 ms remains below 9 kJ g^{-1}. There is only evaporation occurring. Reducing the damage threshold value to 8 kJ g^{-1} keeps the total erosion constant but increases brittle destruction considerably and reduces evaporation down to 10 μm. Now brittle destruction also occurs for 0.5 GW m^{-2}. Brittle destruction under hot plasma impact is not occurring at vertical targets with peak target heat loads up to 30 GW m^{-2} for damage threshold values above 8 kJ g^{-1} [7]. Predamaging of graphite with moderate crack formation might have been occurred during preceding off-normal events. Brittle destruction then finally might develop in the predamaged sample for damage threshold values well below 10 kJ g^{-1} which might result in considerable macroscopic erosion [8].

3. Melt layer erosion of metals

3.1. Simulation experiments

Experimental results from e-beam facilities on melt layer erosion demonstrate the existence of a rather pronounced motion in the melt layer [9,10]. As a result mountains of ejected melt material are formed at the

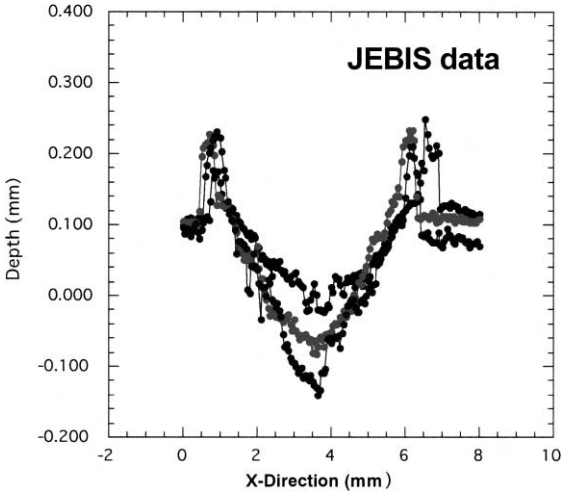

Fig. 3. Typical melt layer erosion profiles for tungsten targets under e-beam impact with 70 keV. The absorbed energy is 2.3 MJ m^{-2}, the time duration of the pulse is 1.8 ms. The initial temperature of the sample is 1000 K.

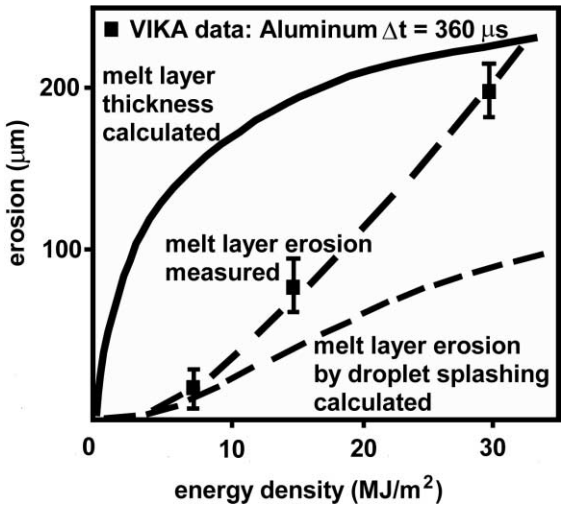

Fig. 4. Melt layer erosion of aluminum under intense pulsed heat loads from plasma streams. Perpendicular impact of unmagnetized plasma stream of duration of 360 μs.

crater edge as is demonstrated in Fig. 3 for tungsten showing typical results for the JEBIS facility [9]. The calculated melt layer thickness without melt flow is 60 μm. Thus the melt flow accounts for an erosion value which is up to a factor of 2.5 larger than the melt thickness without melt flow.

The 1-D shallow water model is used for the calculation of melt layer motion under the external forces surface tension, recoil force of the evaporated metallic atoms and vapor pressure. Melt flow and formation of mountains are obtained in the numerical modelling for tungsten under the JEBIS conditions. However the calculated value of the melt layer erosion is only half of the melt layer thickness. Thus the main driving force of the melt flow in these experiments is not clarified up to now [2].

Mass losses were also determined. For tungsten they account for up to 10% of the total eroded mass. This mass loss mainly is due to droplet splashing occurring as a result of volumetric boiling. Onset of KH instabilities triggered by the tangential flow of the melt is of minor importance. The average mass loss for Be was about 1.5 mg [10]. This accounts for about 25% of the total eroded mass.

Melt layer erosion experiments at plasma gun facilities have been performed for tungsten and aluminum [11,12]. The typical mountains at the crater edge indicate melt motion. In Fig. 4 experimental results on melt layer erosion are shown for aluminum together with the calculated melt layer thickness in case of absence of melt motion. Only at power densities above 80 GW m^{-2} melt motion results in melt layer erosion which is larger than the melt layer thickness. After relief of the pressure of the impacting hot plasma violent boiling with bubble collapse and splashing of melted material occurs. The resulting calculated melt layer erosion by droplet splashing is also shown in Fig. 4. It accounts for up to 50% of the total eroded mass of aluminum. For tungsten droplet splashing accounts for up to 20% of the total eroded mass. The larger fraction of mass loss by droplet splashing under plasma impact is due to the higher power densities used, the larger vapor pressure and the larger contribution of KH instabilities triggered by plasma wind along the target surface.

3.2. Tokamak conditions

The rather strong currents flowing from the plasma to the divertor during hot plasma and RAE impact produce Lorentz forces which considerably contribute to melt motion as was demonstrated in the Be melt experiment at JET for hot plasma impact [13] and in a simulation experiment [14]. The influence of Lorentz forces on melt motion recently was shown in a first numerical simulation of melt motion [2]. In the case of RAE impact eddy currents add to the Lorentz force if the current quench time remains below 100 ms [15] and if the eddy currents are produced well within 20 ms after RAE impact because of resolidification of the melt.

Calculated evaporation and melt layer thicknesses are listed in Table 2 for RAE and hot plasma impact. The temperature-dependent thermophysical data were taken from [16]. Vapor shielding for RAEs and droplet shielding for hot plasma impact are taken into account. A first estimation on dust particle shielding is presented in [7]. Melt motion results in melt layer erosion being up

Table 2
Calculated evaporation and melt layer thickness of tungsten and beryllium for RAEs with an impact energy of 15 MeV and impact angle 1° and for hot plasma impact without melt movement[a]

Impacting particles	Power density in beam (GW m^{-2})	Time duration (ms)	Thickness (μm)			
			Tungsten		Beryllium	
			Melted	Evaporated	Melted	Evaporated
RAEs	0.5	100	1000	15	1800	50
	1.0	50	1050	30	1800	100
	2.5	20	1050	280	1900[b]	100
Hot plasma	30	1	85	0.2		
	3	10	165	0.1		
Hot plasma	0.5	100	350	0.06	190	0.3
	Without shield		850	120	700	500

[a] Vapor shielding for RAEs is taken into account. Initial temperature of FW is 400 K, of vertical target 1000 K.
[b] Volumetric boiling occurs after 16 ms at a depth of 500 μm. As a consequence melt splashing with droplets occurs. However melt motion also occurs and starts earlier. A consistent modelling is required.

to a factor of 2 larger than the melt layer thicknesses given in Table 2. The melt layer erosion thus can be considerably larger than the melt thickness formed during the heat load period. Mass losses by droplet splashing are estimated to be typically 20% for beryllium and 10% for tungsten.

4. Impurity production and transport during ELMs

ELMs when depositing their energy into layers with roughened surfaces might result in enhanced impurity production at hot spots. This might have been experienced at JET when after the Be melt experiment a standard discharge with separatrix strike point (SSP) just at the damaged area ended with a density limit disruption [13]. Hot spot impurity production was analyzed by use of the multifluid 2-D radiation magneto-hydrodynamics (R-MHD) code FOREV-2 [17]. The heat load at the vertical target with inclination angle of 20° was assumed to be 1 GW m^{-2} during 0.5 ms. In this first estimation it is assumed that 10% of the heat deposited area consists of hot spots which then because of energy conservation are heated by 10 times the nominal target heat load. The hot spots in this first estimation are assumed to consist of the same material as the bulk target.

For graphite the heat conductivity was reduced by a factor of 4 to simulate redeposited layers. Fig. 5 shows the calculated evolution of carbon density distributions for densities in the range from 10^{14} to 10^{18} cm^{-3} and the flow pattern (arrows, nv) in the plasma shield of the outer divertor leg of ITER-FEAT. During target heating by the ELM two plasma fans form on either side of the separatrix. After switching off heating the cold dense plasma close to the target surface drifts downstream along the target surface in agreement with the results from simulation experiments with vertical targets [18].

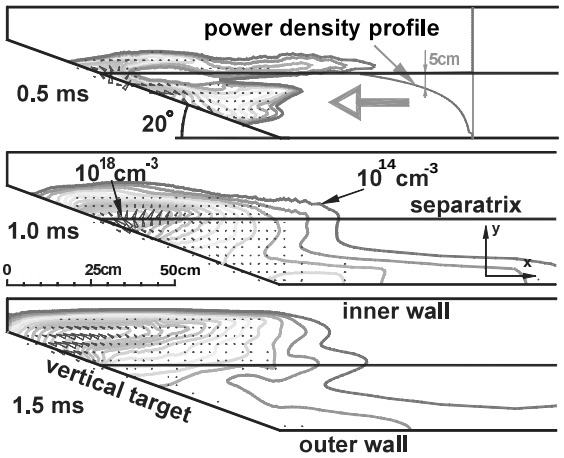

Fig. 5. Impurity production from heating of graphite hot spots during an ELM with an energy of 0.5 MJ m^{-2} and a time duration of 0.5 ms and evolution of carbon densities in the range from 10^{14} to 10^{18} cm^{-3} in the plasma shield and of the plasma flow pattern after the end of heating.

The low-dense plasma with densities up to 10^{15} cm^{-3} moves between the outer wall and the separatrix upwards towards the x-point. In total 2×10^{19} carbon atoms have been evaporated per 1 cm of toroidal length during the ELM. About 25% of them will approach the x-point.

Fig. 6 shows the calculated evolution of tungsten density distributions for the density range from 10^{14} to 10^{17} cm^{-3} and of the flow pattern in the plasma shield. During heating the tungsten plasma shield shows a pronounced downstream drift along the target surface. After switching off heating a weak downstream drift continues but the plasma now mainly moves close to the separatrix upwards towards the x-point. The total

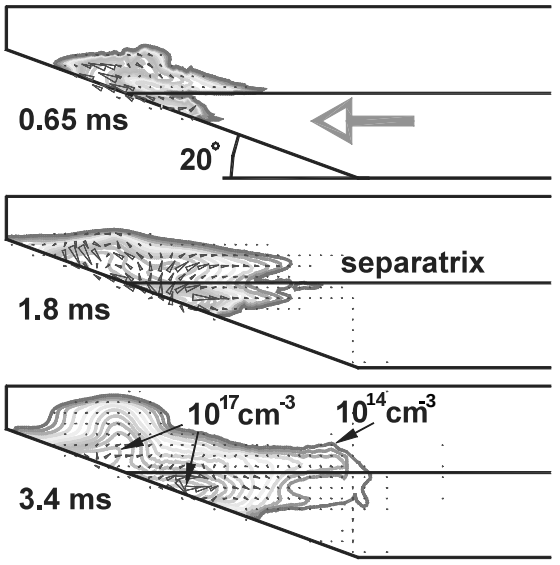

Fig. 6. Impurity production from heating of tungsten hot spots during the same ELM as of Fig. 5 and evolution of tungsten densities in the plasma shield and of the flow pattern after the end of heating.

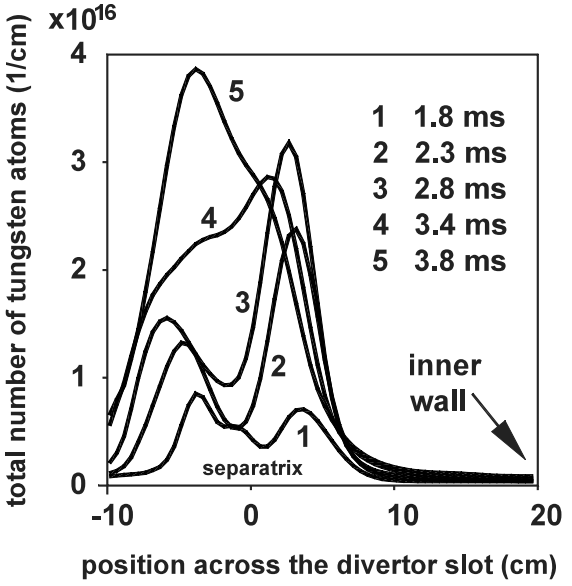

Fig. 7. Time evolution of the total number of tungsten atoms across the outer divertor leg within 0.3 to 1.2 m distance from the SSP per 1 cm of toroidal length. The outer wall is at −20 cm.

number of tungsten atoms between 0.3 and 1.2 m distance from the SSP per 1 cm of toroidal length is shown in Fig. 7. 8×10^{17} tungsten atoms have been evaporated and after 5 ms about 2×10^{17} atoms are approaching the ITER-FEAT x-point. The graphite and tungsten ion/neutral fluxes close to the x-point typically are 6.5×10^{22} and 1.2×10^{20} cm^{-2} s. In total 6×10^{20} tungsten atoms and 10^{22} carbon atoms are reaching the x-point. These neutrals both have the potential to dissipate a considerable fraction of the thermal energy of the central plasma. Therefore an ELM energy of 0.5 MJ m^{-2} under the hot spot conditions as described is hardly tolerable.

5. Conclusions

Brittle destruction of graphite under RAE impact produces rather large amounts of dust. Graphite as FW material thus causes safety problems. Brittle destruction of dump plates under hot plasma impact could be of concern if fatigue effects could reduce the damage threshold which was determined for volumetric energy deposition. Melt layer erosion of metals under RAE impact is dominated by melt flow. The erosion value is up to a factor of 2 larger than the melt thickness. The driving force behind the melt flow is unclear. Erosion of tungsten FWs can be up to 2 mm, for Be up to 3.5 mm for RAE impact. Due to the large damage for RAEs it is mandatory to mitigate those events or to limit the tolerable RAE energy density to values below 20 MJ m^{-2}. In this case brittle destruction of graphite with 10 kJ g^{-1} will not occur too but occurs for power densities above 1 GW m^{-2} for 8 kJ g^{-1}. Due to the considerable implications of melt motion on melt layer erosion more experimental and theoretical investigations on this topic are urgently required. Melt layer erosion always is accompanied by splashing. Up to 20% of the eroded mass is splashed away by droplets. Flaking from redeposited layers, dust, melt flow and droplet splashing during disruptions produce complex layers with considerable surface roughness and drastically changed thermophysical properties. The hot spots of such layers are responsible for enhanced impurity production. A characterization of such layers is urgently required. First numerical estimations show that the maximum tolerable ELM energy is noticeably lower for redeposited layers with considerable surface roughness than for the virgin vertical target.

References

[1] V.T. Astrelin et al., Nucl. Fus. 37 (11) (1997) 1541.
[2] I. Landman, H. Würz, FZKA Report 6517, 2000.
[3] L.D. Horton, in: Proceedings of the 24th EPS Conference on Controlled Fusion and Plasma Physics, Berchtesgaden, 9–13 June 1997, vol. 21A, Part I, p. 65.
[4] A.W. Leonard et al., J. Nucl. Mater. 266–269 (1999) 109.
[5] K. Nakamura et al., J. Nucl. Mater. 212–215 (1994) 1201.
[6] M. Guseva et al., in: Proceedings of the 12th International Conference on Ion Surface Interaction, Moscow, 1995, vol. 1, p. 130.

[7] H. Würz et al., in: Proceedings of the 27th EPS Conference on Controlled Fusion and Plasma Physics, Budapest, 12–16 June 2000.
[8] S. Pestchanyi et al., FZKA Report 6466, 2000.
[9] K. Nakamura et al., J. Nucl. Mater. 233–237 (1996) 730.
[10] A. Lodato et al., in: Paper at ISFNT-5, Rome, September 1999, Fus. Eng. Des. (to be published).
[11] V.G. Belan et al., Fus. Technol. 1 (1998) 101.
[12] V.N. Litunovsky et al., Fus. Eng. Des. 39–40 (1998) 303.
[13] B.J.D. Tubbing et al., in: Proceedings of the 22nd EPS Conference on Controlled Fusion and Plasma Physics, Bournemouth, vol. 19C, Part III, p. 453.
[14] H. Madarame et al., Fus. Eng. Des. 18 (1991) 109.
[15] H. Hashizuma et al., Fus. Eng. Des. 9 (1989) 219.
[16] R. Hultgren, ASM Metals, Park Ohio, 1973.
[17] H. Würz et al., FZKA Report 6198, 1999.
[18] N. Arkhipov et al., in: Proceedings of the 26th EPS Conference on Controlled Fusion and Plasma Physics, Maastricht, Netherlands, 1999.